Experimental Measurement of Electron Particle Diffusion from Sawtooth-Induced Density-Pulse Propagation in the Texas Experimental Tokamak

S. K. Kim, D. L. Brower, W. A. Peebles, and N. C. Luhmann, Jr.
Institute of Plasma and Fusion Research, University of California, Los Angeles, California 90024
(Received 17 September 1987)

Electron density perturbations produced by sawtooth oscillations in the interior of the Texas Experimental Tokamak are measured with a high-resolution, multichannel, far-infrared interferometer. Abel inversion over the sawtooth perturbation indicates a space-time evolution which is diffusive in character. The diffusion coefficient is determined from a density-pulse–propagation model and found to be appreciably larger than equilibrium values.

PACS numbers: 52.55.Fa, 52.35.Kt, 52.35.Mw

Since first being observed on the ST tokamak,[1] sawtooth oscillations, which are sometimes referred to as "minor" or "internal" disruptions, have remained an active research area. This stems primarily from their dominance of transport inside the inversion radius (i.e., $r_{q=1}$, where q is the safety factor) and their usefulness in providing a direct measure of the radial electron thermal-conduction coefficient. As the electron heat conduction in tokamaks is observed to be anomalous, this is an issue of critical importance. Consideration of the sawtooth as a naturally occurring perturbation in the plasma temperature allows the heat transport properties of the background plasma to be deduced from its propagation characteristics through the tokamak confinement zone[2,3] (i.e., the region outside $r_{q=1}$ and inside the edge). From such an analysis, it has generally been determined that sawtooth-induced heat-pulse propagation is completely diffusive. However, the measured electron thermal diffusivity (χ_e) from heat-pulse propagation can be a few times larger than the value inferred from power-balance calculations.[4-6] The discrepancy between heat-pulse and power-balance observations has been attributed to both physical effects[4,7-9] and to basic differences in the measured quantities.[5,10] Physical understanding of the sawtooth phenomenon has been complicated by recent observations (e.g., double or giant sawteeth, fast collapse, no $m=1$ precursor) on several tokamaks [Doublet III,[11] Joint European Torus,[12,13] Texas Experimental Tokamak (TEXT),[14,15] and Tokamak Fusion Test Reactor[16]] which indicate that the Kadomtsev model[17] may be inadequate. From these unresolved issues it is clear that many questions regarding the plasma sawtooth oscillation are left unanswered.

All heat-pulse–propagation experiments assume the effect of the internal sawtooth disruption on the plasma density to be negligible, with the associated heat flux being primarily due to electron thermal conduction. However, in this Letter, we report results from a high-sensitivity ($\simeq 5\times10^{10}$ cm^{-3}), high spatial (3 cm) resolution, multichannel, far-infrared interferometer on TEXT which has measured the effects of sawtooth disruptions on the electron density from plasma interior to edge regions. These measurements provide new information on sawtooth-induced density-pulse propagation. Specifically, the experimental observations are consistent with a diffusive model and permit the associated electron particle diffusion coefficient to be determined. Data analysis is analogous to standard heat-pulse propagation measurements.[2-4] For the discharges studied, the density perturbation is $\Delta n_{st}/n_e \simeq (3\text{–}5)\%$ at the mixing radius with the spatially averaged diffusion coefficient in the confinement region measured to be $D_e \simeq 2\text{–}5$ m^2/s, several times larger than equilibrium values. This anomaly is comparable to that for the heat-pulse analog under similar conditions.[4,6] These results have fundamental new implications for tokamak heat-flux measurements, for coupling between heat and particle transport, and for the physical understanding of sawtooth mechanisms.

Details of the multichannel, heterodyne, far-infrared laser interferometer system are described by Peebles *et al.*[18] The twin-frequency laser source operates at 432 μm ($\simeq$60 mW) with an IF frequency of $\simeq$750 kHz. Both the probe and local oscillator beams are expanded in one dimension via parabolic cylindrical mirrors in order to view the entire plasma cross section accessible from the viewing ports. High spatial sampling is achieved by the arrangement of twelve (12) corner-cube GaAs Schottky-diode mixers in a linear array with a spacing of 3 cm from the plasma outside edge to center. The receiver system is sensitive to density perturbations of $\simeq 5\times10^{10}$ cm^{-3}, allowing observation of sawtooth phenomena and Mirnov oscillations; measurement of $m=1$ and higher-order modes is possible.[18] Data are taken during the plateau region of Ohmic discharges on TEXT whose major radius is $R=1$ m and limiter radius is $a=26$ cm.

In Fig. 1, the chord-averaged density $\bar{n}_e$ is plotted for vertical chords positioned from $R=88$ to 124 cm for the discharge $I_p=300$ kA, $B_T=2.0$ T, and $\bar{n}_{e0}=4\times10^{13}$ cm^{-3}, where I_p, B_T, and $\bar{n}_{e0}$ correspond to the plasma current, toroidal field, and central chord-averaged density, respectively. The internal disruptions inside the in-

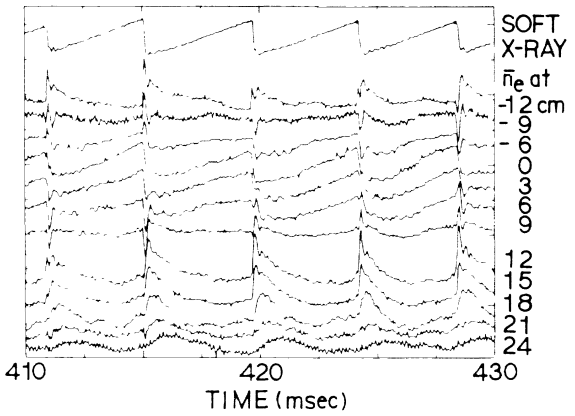

FIG. 1. Chord-averaged interferometer signals (12 channels) taken from the plateau region of a discharge whose parameters were $I_p = 300$ kA, $B_T = 2.0$ T ($q_a = 2.3$), and $\bar{n}_{e0} = 4 \times 10^{13}$ cm^{-3}. Scaling factors are the same for each trace. Density sawteeth are in phase with the central soft-x-ray signal. The temporal variation in the signals (sharp fall inside, sharp rise outside) shows that $r_{q=1} \simeq 9$ cm.

version radius are manifested by an abrupt decrease in the chord-averaged density as particles are rapidly lost from the central region, followed by a slower recovery, giving rise to the characteristic sawtooth behavior. This process, which will not be discussed in detail, results in a pulse of particles being ejected into the volume immediately outside the inversion radius where the sawtooth oscillation is inverted with respect to the inside. The picture described above is completely analogous to the heat-pulse counterpart and suggests a coupling between the two phenomena.[7,8]

An Abel inversion is performed to arrive at the local sawtooth density-perturbation profile. In order to minimize errors near the crash where $m = 1$ oscillations are often large, a numerical boxcar averaging technique is applied during the plateau region of the discharge where the sawtooth period and amplitude are essentially constant. The Abel-inverted, density-sawtooth time history is shown in Fig. 2(a) at various positions outside the inversion radius ($r_{q=1} \simeq 9$ cm). Important features to note are the broadening of the pulse towards the plasma edge and the increasing delay of the peak time with minor radius, thereby creating the image of pulse propagation. Figure 2(b) follows the evolution of the density-perturbation profile during a sawtooth cycle. Here, it is clearly observed that immediately after the sawtooth crash ($t \simeq 0.1\tau_{st}$, where τ_{st} is the sawtooth period), electrons ejected from the central region are deposited at radius $r \simeq 13$ cm, which corresponds to the mixing radius (roughly given by $r_{mix} \simeq \sqrt{2} r_{q=1}$). The magnitude of the peak in the perturbation profile subsequently decays but the position remains stationary throughout the duration of the cycle. Behavior at the edge is complicated as a result of source effects. Development of the sawtooth per-

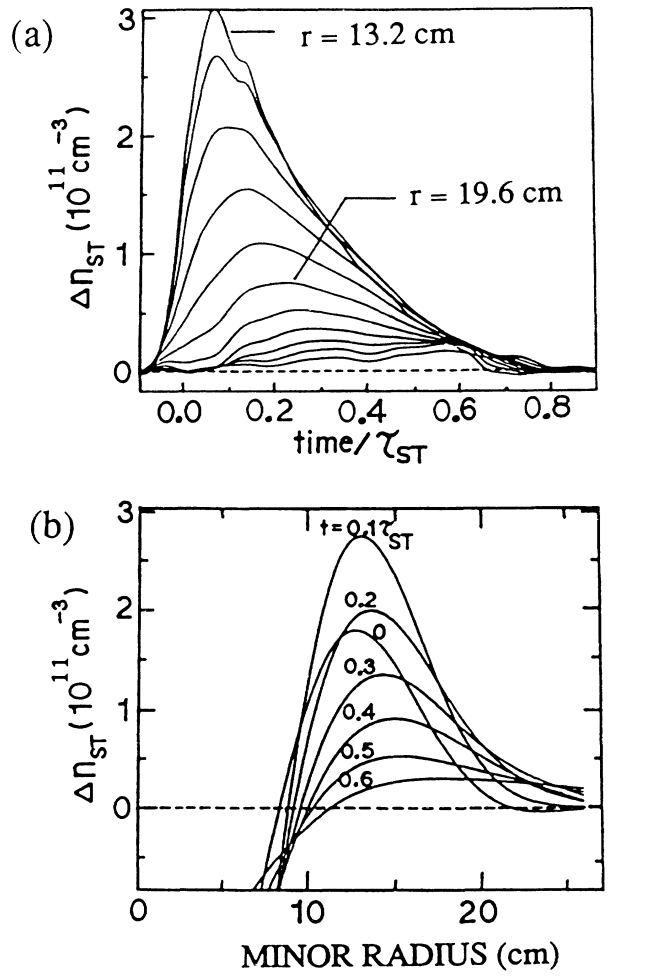

FIG. 2. (a) Abel-inverted sawtooth time history plotted with decreasing amplitude for equal radial increments of $\Delta r = 0.3$ cm from $r = 13.2$ to 26.2 cm. Note the roughly exponential falloff in the region $r = 13$–18 cm. (b) Profile evolution of the sawtooth density perturbation with t/τ_{st} ranging from 0 to 0.6. Time zero is taken at the midpoint of the crash. $I_p = 300$ kA, $B_T = 2.0$ T, $\bar{n}_{e0} = 1.7 \times 10^{13}$ cm^{-3}.

turbations outside the inversion radius strongly suggests that a diffusive process is dominating the particle transport. There is no evidence for ballistic or wave propagation. For the discharges studied, the perturbation level increases linearly with $\bar{n}_{e0}$ maintaining a normalized fluctuation level $\Delta n_{st}/n_e \simeq (3$–$5)\%$, at the mixing radius. A maximum perturbation occurs at the plasma center where $\Delta n_{st}/n_e \simeq (6$–$10)\%$, a value of the same order as the temperature perturbation.

The pulse-propagation characteristics discussed in the preceding paragraphs can be described by a simple theoretical model based on the particle continuity equation:

$$\partial n/\partial t = \nabla \cdot (D_e \nabla n - n v_p) + S(r,t), \quad (1)$$

where $S(r,t)$ is the plasma source including ionization

and recombination, and the radial particle flux $\Gamma(r,t) = D_e \nabla n - n v_p$, with D_e being the electron diffusion coefficient and v_p the inward pinch velocity. The analysis is restricted to the confinement region allowing the source term to be neglected. The inward pinch exists during the sawtooth cycle as evidenced by the density channels inside the inversion radius after the sawtooth crash (see Fig. 1). However, the overall density-perturbation development outside the inversion radius appears to be diffusion dominated [see Fig. 2(b)]. Therefore, for $r > r_{q=1}$, we assume that the transport can be represented by a diffusive process, reducing Eq. (1) to

$$\partial n/\partial t = \nabla \cdot [D_e \nabla n]. \quad (2)$$

This is completely analogous to Eq. (2) of Ref. 2, where

$$\partial(\tfrac{3}{2} n T_e)/\partial t = \nabla \cdot [n \chi_e \nabla T_e] \quad (3)$$

for the equivalent heat-pulse analysis. When solving Eq. (3), density is treated as a constant in space and time during the sawtooth cycle,[2-4] an assumption which may need to be critically reevaluated in light of the present results. In the present analysis, solution of Eq. (2) is made with the initial condition of a density perturbation given by a dipole particle source and follows directly after that of Fredrickson *et al.*[4] where the transport coefficient is treated as a constant. The resulting maximum density perturbation at a given radius r occurs at time $t_p(r) = r^2/12D_e$, with magnitude $\Delta n_{st}(r, t_p(r))$ falling off as r^{-4}.

Comparison of the diffusive model with experimental data is shown in Fig. 3. The linear dependence between t_p and r^2 is seen in Figs. 3(a) and 3(b), at various plasma densities for discharges with $q_a = 3.5$ and 2.3, respectively. The slope changes with q_a but remains essentially constant with changing plasma density. Deviations from an asymptotic dependence on r^2 occur at either extreme of the confinement region. Similarly, the maximum density perturbation decreases as r^{-4} under a variety of plasma conditions, as shown in Fig. 3(c). The structure observed near the edge may be due to source effects or a spatially varying diffusion coefficient. On all points of comparison with the diffusive model, reasonable agreement with experimental data is obtained, suggesting that the assumptions made in arriving at Eq. (2) are justified. This is further supported by the data in Fig. 2(b). Models describing wave propagation [which contradicts Fig. 2(a)] or ballistic motion [which contradicts Fig. 2(b)] of the perturbation deviate substantially from the experimental observations. Thus, we conclude that density pulses produced by internal disruptions (i.e., sawteeth) propagate out through the confinement region of TEXT in a manner consistent with a diffusive process.

The electron particle diffusion coefficient can be calculated from the solution of Eq. (2) with use of data in Fig. 3. For the discharges discussed, the average diffusion

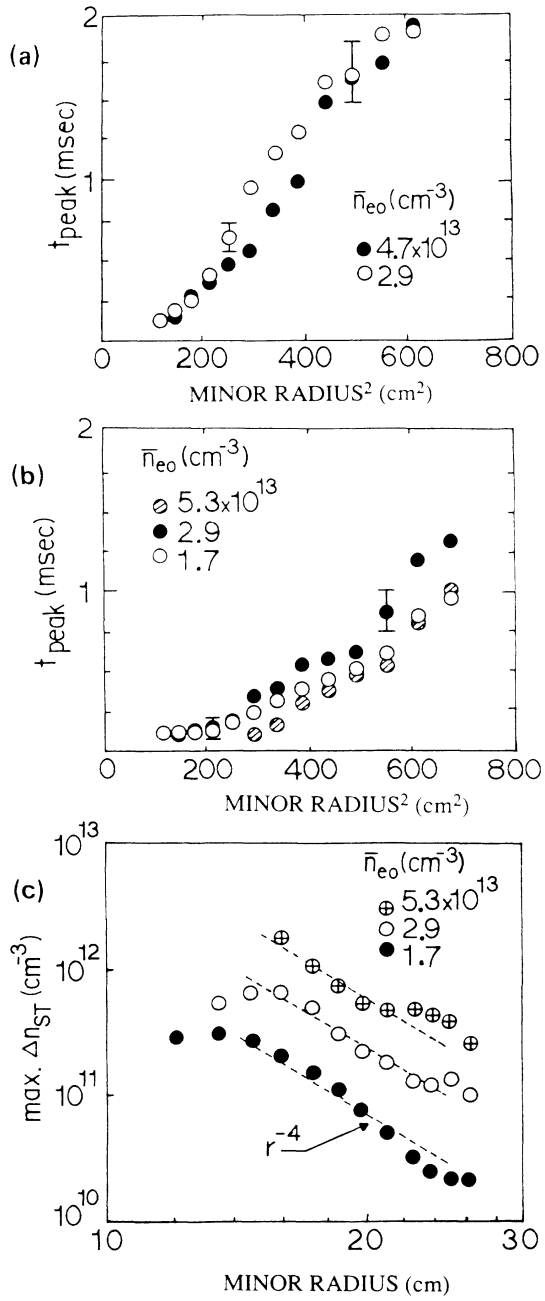

FIG. 3. Comparison of data with the diffusive model. (a),(b) Peak arrival time vs radial position for $q_a = 3.5$ and 2.3, respectively. The slope asymptote is $\simeq (12D_e)^{-1}$ and thus provides a measure of D_e. (c) Maximum Δn_{st} as a function of radius. Note r^{-4} falloff at all densities. $I_p = 300$ kA, $B_T = 2.0$ T.

coefficient in the confinement region is 2.1 m^2/s (5.5 m^2/s) for $q_a = 3.5$ (2.3). The diffusion coefficient appears insensitive to density [see Figs. 3(a) and 3(b)] and varies inversely with q_a as shown in Fig. 4. These values are 2–5 times larger than those estimated from oscillating-gas-puff experiments[19] which are more indicative of an equilibrium situation as the perturbation cycle is

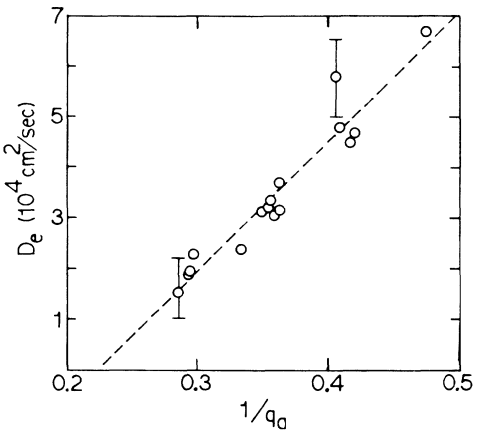

FIG. 4. Scaling of the particle diffusion coefficient, as measured from sawtooth density-pulse propagation, with the safety factor ($q_a = aB_T/RB_p$).

roughly 5 times greater than the global energy confinement time. The density-pulse diffusion coefficient is approximately equal to the electron thermal diffusivity measured via heat-pulse-propagation techniques, which is a factor of 3 larger than power-balance results.[6] Pulse-propagation models tend to overestimate the transport coefficients,[10] although not by the large factors observed in these measurements.

It has been surmised that the differences between perturbative measurements of the transport coefficients and equilibrium values may be driven by electrostatic or magnetic fluctuations.[4] Preliminary attempts to correlate density-fluctuation measurements with sawtooth oscillations on TEXT[20] indicate a prompt burst of microturbulence activity during the crash at which time the scattered power can more than double. Enhanced turbulence has been observed to persist the entire time necessary for the density pulse to pass (t_p), although this is not always the case. Modifications to the frequency and wave-vector spectra during the sawtooth cycle are presently under active investigation. Recent theoretical works by Hossain *et al.*[7] and Stockdale, Burrel, and Tang[8] claim that the anomaly between equilibrium and perturbation measurements can be resolved by an examination of the coupling of heat flow and plasma diffusion. The density-pulse-propagation measurements presented in this paper strongly suggest that particle diffusion may play an important role in sawtooth heat transport. In addition, the steady-state case may contain an appreciable inward particle pinch which could account for the disparity between equilibrium and perturbative measurements of the electron diffusion coefficient. This argument has already been proposed to explain the analogous discrepancy observed for the electron thermal diffusivity.[4,9]

In conclusion, the electron density perturbations produced by sawtooth phenomena are found to have a clearly diffusive space-time evolution and the associated transport coefficient is anomalously large when compared to equilibrium values. From analogies between density- and heat-pulse-propagation measurements, a coupling can be inferred which implies that particle and heat diffusion should no longer be treated separately for sawteeth. Future experiments will detail the comparison between the density and temperature perturbations, their transport coefficients, and electrostatic density fluctuations.

Helpful discussions with P. H. Diamond and K. W. Gentle and the technical support of the TEXT staff are gratefully acknowledged. This work is supported by the U.S. Department of Energy under Contract No. DE-AC05-78ET53043.

[1]S. Von Goeler, W. Stodiek, and N. Sauthoff, Phys. Rev. Lett. **33**, 1201 (1974).

[2]J. D. Callen and G. L. Jahns, Phys. Rev. Lett. **38**, 491 (1977).

[3]M. Soler and J. D. Callen, Nucl. Fusion **19**, 703 (1979).

[4]E. Fredrikson *et al.*, Nucl. Fusion **26**, 849 (1986).

[5]B. J. D. Tubbing and N. J. L. Cardozo, Joint European Torus Report No. JET-R(87)01, 1987 (to be published).

[6]S. B. Kim, T. P. Kochanski, and E. J. Powers, Bull. Am. Phys. Soc. **30**, 1568 (1985).

[7]M. Hossain *et al.*, Phys. Rev. Lett. **58**, 487 (1987).

[8]R. E. Stockdale, K. H. Burrel, and W. Tang, Bull. Am. Phys. Soc. **31**, 1535 (1986).

[9]J. D. Callen *et al.*, Joint European Torus Report No. JET-P(87)10, 1987 (to be published).

[10]W. J. Goedheer, Nucl. Fusion **26**, 1043 (1986).

[11]W. Pfieffer, Nucl. Fusion **25**, 673 (1985).

[12]D. J. Campbell *et al.*, Nucl. Fusion **26**, 1085 (1986).

[13]A. W. Edwards *et al.*, Phys. Rev. Lett. **57**, 210 (1986); J. Wesson *et al.*, Plasma Phys. Controlled Fusion **28**, 243 (1986).

[14]S. B. Kim, Nucl. Fusion **26**, 1251 (1986).

[15]J. A. Snipes and K. W. Gentle, Nucl. Fusion **26**, 1507 (1986).

[16]G. Taylor *et al.*, Nucl. Fusion **26**, 339 (1986).

[17]B. B. Kadomtsev, Fiz. Plazmy **1**, 710 (1975) [Sov. J. Plasma Phys. **1**, 389 (1975)].

[18]W. A. Peebles *et al.*, to be published.

[19]K. W. Gentle, B. Richards, and F. Waelbroeck, Plasma Phys. Controlled Fusion **29**, 1077 (1987).

[20]D. L. Brower *et al.*, in *Proceedings of the Fourteenth European Conference on Controlled Fusion and Plasma Physics, Madrid, Spain, 1987,* edited by S. Methfessel (European Physical Society, Petit-Lancy, Switzerland, 1987), Vol. 11D, Pt. III, pp. 1314–1317.